Immune synapses between mast cells and γδ T cells limit viral infection

Chinmay Kumar Mantri[1] and Ashley L. St. John[1,2,3]

[1]Program in Emerging Infectious Diseases, Duke–National University of Singapore (Duke-NUS) Medical School, Singapore. [2]Department of Pathology, Duke University Medical Center, Durham, North Carolina, USA. [3]Department of Microbiology and Immunology, Young Loo Lin School of Medicine, National University of Singapore, Singapore.

Mast cells (MCs) are immune sentinels, but whether they also function as antigen-presenting cells (APCs) remains elusive. Using mouse models of MC deficiency, we report on MC-dependent recruitment and activation of multiple T cell subsets to the skin and draining lymph nodes (DLNs) during dengue virus (DENV) infection. Newly recruited and locally proliferating γδ T cells were the first T cell subset to respond to MC-driven inflammation, and their production of IFN-γ was MC dependent. MC–γδ T cell conjugates were observed consistently in infected peripheral tissues, suggesting a new role for MCs as nonconventional APCs for γδ T cells. MC-dependent γδ T cell activation and proliferation during DENV infection required T cell receptor (TCR) signaling and the nonconventional antigen presentation molecule endothelial cell protein C receptor (EPCR) on MCs. γδ T cells, not previously implicated in DENV host defense, killed infected targeted DCs and contributed to the clearance of DENV in vivo. We believe immune synapse formation between MCs and γδ T cells is a novel mechanism to induce specific and protective immunity at sites of viral infection.

Introduction

Mast cells (MCs) are tissue-resident cells that are distributed throughout the dermis, where they have an evolutionarily conserved responsibility to the host for pathogen surveillance (1). Although MCs have long been associated with pathological conditions including asthma and allergy (2), they are also now well accepted as sentinel cells that send an alarm to the immune system that a pathogen is present. MCs perform this task efficiently and recognize multiple classes of pathogens by detecting bacterial or viral structural components using a wide range of traditional pathogen-associated molecular patterns (e.g., TLRs) (3). MCs are also activated by indirect, endogenous signals of infection (such as those to complement) (1). When activated, MCs respond in a biphasic manner, within seconds releasing preformed mediators that are packed tightly into granules, while initiating proinflammatory transcriptional programs. The second phase of the response involves release of these de novo–produced cytokines and chemokines in the hours following activation (1). MC innate responses to pathogens promote pathogen clearance in vivo through initiation of inflammation and recruitment and activation of other immune cells within the site of infection. Although MCs are well known to play a role in host defense against bacteria and parasites, MC responses to viral pathogens had hardly been examined until recently (1, 4). MCs degranulate highly in response to dengue virus (DENV), a clinically relevant *Flavivirus* that infects the skin after a mosquito bite. DENV activation of MCs promotes immune clearance of DENV in the skin and in draining lymph nodes (DLNs), which is characterized by the recruitment of cytotoxic lymphocytes, such as NK cells and NKT cells, to DENV infection sites by MCs (5). This raises the question of whether other subtypes of lymphocytes are recruited to the peripheral sites of infection by MCs and what functional impact this interaction could have on viral clearance.

There is increasing evidence of MC interaction with T cells in tissues. For example, in addition to NKT cell recruitment during DENV infection, it has been shown that MCs promote the recruitment of $CD8^+$ T cells during Newcastle virus infection (6). MCs responding to viral pathogens have been shown to produce several chemokines that are understood to promote the recruitment of various subsets of T cells, including CCL5, CXCL10, CXCL12, and CX3CL1 (5–7). In addition to directing chemotaxis, MCs also prompt endothelial activation, which is required for extravasation from the blood vessel lumen into tissues (8). An important component of this is MC-derived TNF, which induces E-selectin expression on vascular endothelium (9). Aside from cellular recruitment, MCs could potentially influence T cell responses through other mechanisms. For example, MC-derived preformed TNF is required for the LN hypertrophy (retention of B and T cells in LNs) that occurs in the hours after acute inflammation is initiated (10). This response is thought to be essential for optimal immune specificity, since it increases the probability that rare antigen-specific T cells are present in DLNs as the adaptive immune response is undergoing refinement.

Given the discordant results from in vitro and in vivo studies (11), the question of whether MCs are physiologically relevant as antigen-presenting cells (APCs) remains unanswered. Our understanding is further obstructed by the fact that MCs provoke antigen-independent activation of T cells in coculture experiments (12, 13), so whether antigen presentation in a traditional sense occurs has remained unclear. MCs do not constitutively

Conflict of interest: The authors have declared that no conflict of interest exists.

Submitted: May 29, 2018; **Accepted:** December 11, 2018.
Reference information: *J Clin Invest*. 2019;129(3):1094–1108.
https://doi.org/10.1172/JCI122530.

express MHC class II molecules on their surface in the skin, although MHC class II is inducible on MCs in various inflammatory and experimental contexts (14). MCs also express some nonclassical MHC molecules, such as CD1d (15). Despite the divergent data regarding whether MCs can serve as APCs in vivo, there is a consensus that MCs have been described to physically interact with T cells in tissue sections (16), but the function and mechanisms of this interaction remain unknown.

Aside from MCs, other immune cells reside in peripheral tissues and contribute to innate immune responses. For example, γδ T cells patrol the skin, although not much is known about their function in immune responses and the mechanisms that lead to their activation (17, 18). However, γδ T cells have been implicated in the clearance of West Nile virus infection (19, 20), which is closely related to DENV and also injected into the skin by mosquitos. Typically, γδ T cells are not restricted to the recognition of antigen bound to MHC molecules (17), and these T cells have the ability to become activated by certain stimuli completely independent of antigen presentation (21), suggesting that they may not need signals from other cells or contact with them to become activated. Both γδ T cells and MCs inhabit the same peripheral milieu, both cell types function as a bridge between innate and adaptive immunity, and both are responsible for host defense and pathogen clearance. However, to our knowledge, interactions between MCs and γδ T cells have not been reported or postulated.

In this study, we sought to understand the contributions of MCs to the trafficking and activation of various T cell subsets in the skin during acute viral infection. Our data show that not only are MCs consequential to the regulated trafficking of multiple subsets of T cells during viral infection, but they also contribute significantly to the early recruitment, activation, and proliferation of γδ T cells through the nonconventional antigen presentation molecule endothelial cell protein C receptor (EPCR), in a γδ T cell receptor (γδ TCR) signaling-dependent manner involving immune synapse formation. In turn, γδ T cells enhance the clearance of virus in vivo, emphasizing the functional significance of the physical interaction between MCs and γδ T cells.

Results

MCs recruit multiple subsets of T cells to viral infection sites. To investigate the role of MCs in potentiating T cell responses during cutaneous viral infection, we injected 1×10^5 pfu DENV2 s.c. into the footpad (FP) skin of MC-sufficient C57Bl/6 mice and congenic MC-deficient *Kit*$^{W\text{-}sh/W\text{-}sh}$ (Sash) mice, which have an inversion in the *c-Kit* promoter that impedes development of the MC lineage (22). We infected mice by peripheral injection to replicate the natural route of infection for DENV in humans. The skin of the FPs was removed and processed to single-cell suspensions and stained for flow cytometry using a panel of antibodies designed to identify various subsets of T cells at the site of infection (Supplemental Figure 1; supplemental material available online with this article; https://doi.org/10.1172/JCI122530DS1). Previously, we showed that DENV induces strong MC degranulation in vivo, with approximately 30% of MCs losing granularity in the skin following infection and recruitment of NK and NKT cells into the skin (5), but the responses of additional T cell subsets were not evaluated. Here, when FPs were infected with DENV, we observed that multiple subsets of T cells were enriched in the skin in a MC-dependent manner (Figure 1, A–E). The subsets of T cells dominating the early cutaneous response were innate T cells, including NKT cells (Figure 1B) and γδ T cells (Figure 1C). CD8$^+$ T cells also showed MC-dependent enrichment, but at the later time point of day 3 after infection (Figure 1D), while CD4$^+$ T cells were not enriched significantly in the skin of MC-sufficient mice over MC-deficient Sash mice until day 5 after infection (Figure 1E). Reconstitution of Sash mice (referred to hereafter as Sash-R mice) with bone marrow–derived MCs (BMMCs) resulted in restored recruitment of total T cells, and the numbers of NKT, γδ, CD4$^+$, and CD8$^+$ T cell subsets in the skin were also restored to the levels seen in DENV-infected WT mice (Supplemental Figure 2, A–E), confirming the MC dependency of various subsets of T cells during DENV infection. Furthermore, when we measured the activation status of the recruited T cells, we found that day 3 was a critical time point for T cell activation in the FP following DENV infection. In Sash mice lacking MCs, we observed substantially reduced activation of CD8$^+$, NKT, and γδ T cells at the site of infection compared with WT and Sash-R mice (Figure 1, F–H). In contrast, we found that activation of CD4$^+$ T cells was not influenced by MCs (Figure 1I). Importantly, these defects in T cell recruitment were observed in the skin of Sash mice compared with that of WT and Sash-R mice, even though viral titers were higher in Sash mice than in WT or Sash-R mice, suggesting that this deficit was not due to the lower viral burden in Sash mice (Figure 1J and Supplemental Figure 2F). Together, these data demonstrate that T cell recruitment and activation at the site of cutaneous DENV infection were MC dependent and occurred in response to stimuli from MCs.

MCs induce the retention and activation of T cells in DLNs. The arrival of activated DCs and sequestration of T cells from the circulation that occur during LN hypertrophy provide an optimal environment for the initiation of adaptive immune responses by increasing the likelihood of T cell encounters with their DC-presented cognate antigens (23). Since DENV has been shown to induce a strong degranulation response in MCs and since particulate TNF released by MCs is a potent inducer of LN hypertrophy, we investigated which subsets of T cells were retained in the popliteal LN, which is the DLN for the FP skin (Figure 2). Although we observed retention of multiple subsets of T cells in the DLNs of DENV-infected Sash mice, the magnitude of the total T cell response was significantly lower in comparison with that seen in WT mice, indicating that a significant portion of this response is due to the involvement of MCs in immunosurveillance for DENV (Figure 2A). T cell subsets with innate functions, including NKT cells and γδ T cells, were recruited to DLNs in enhanced numbers in WT mice compared with Sash mice (Figure 2, B and C) and showed significantly increased levels of activation (Figure 2, D and E) at multiple postinfection time points. We also observed a MC-dependent increase in the total numbers and activation of CD8$^+$ T cells 24 hours and 48 hours after infection in WT mice compared with Sash mice (Figure 2, F and G), which is consistent with LN hypertrophy and initiation of adaptive responses against DENV. Moreover, the total numbers of CD8$^+$ T cells were significantly higher in WT mice compared with those in Sash mice at various postinfection time points (Figure 2F). Similarly, CD4$^+$ T cell numbers were higher throughout the time course in WT mice

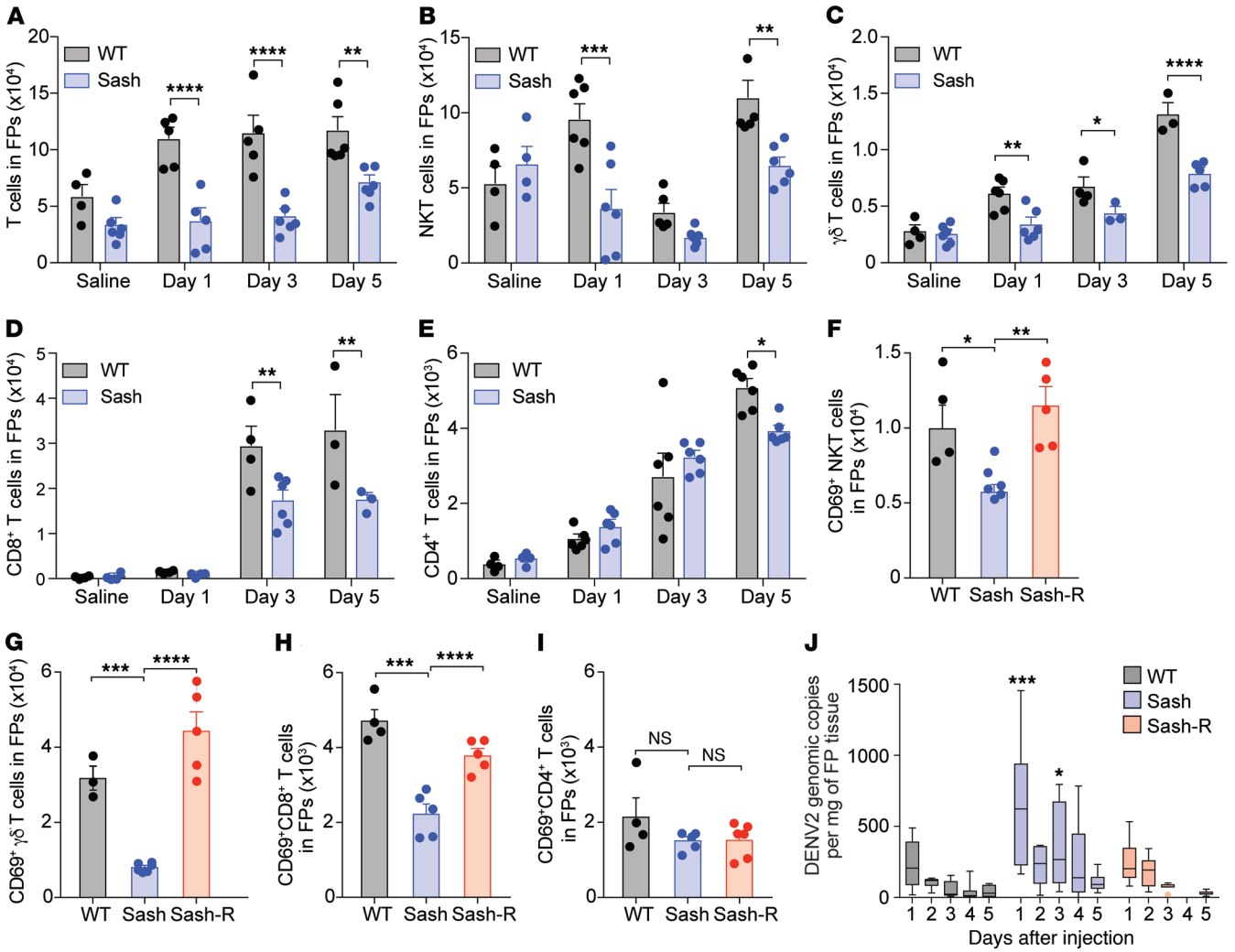

Figure 1. MC-dependent recruitment and activation of T cells in the skin during DENV infection. MC-deficient (Sash) and MC-sufficient (WT) mice were injected with saline or infected with 1×10^5 pfu DENV by s.c. injection into the FP to determine whether T cells were recruited in a MC-dependent fashion during infection. FP skin was collected on days 1, 3, and 5 after infection and dissociated with collagenase to make single-cell suspensions, which were stained for various subsets of T cells prior to flow cytometric analysis (Supplemental Figure 1). Numbers of (**A**) total T cells (CD3⁺), (**B**) NKT cells (CD3⁺NK1.1⁺), (**C**) γδ T cells (CD3⁺γδ TCR⁺), (**D**) CD8⁺ T cells (CD3⁺CD8⁺), and (**E**) CD4⁺ T cells (CD3⁺CD4⁺) were compared between WT and Sash mice. Sash mice reconstituted with BMMCs (Sash-R) were similarly infected, and FP skin cells were stained on day 3 after infection. Reconstitution of MCs in Sash mice restored the deficiency in T cell numbers (Supplemental Figure 2, A–E). In multiple T cell subsets, (**F**) NKT cells, (**G**) γδ T cells, and (**H**) CD8⁺ T cells, (**I**) but not CD4⁺ T cells, there were greater numbers of activated (CD69⁺) T cells in the FPs of WT mice compared with those of Sash mice on day 3 after infection, and the deficiency in activation was repaired in Sash-R mice. (**J**) A larger number of genomic copies of DENV were detected in the FPs of Sash mice compared with those of WT and Sash-R mice, as determined by RT-PCR. The means are depicted by box and whisker plots with Tukey's test error bars. An alternate presentation of the data from **J** showing individual mouse values is provided in Supplemental Figure 2F. For all panels, unless otherwise noted, data represent the mean ± SEM. $^*P < 0.05$, $^{**}P < 0.001$, $^{***}P < 0.001$, and $^{****}P < 0.0001$, by 2-way ANOVA with Sidak's multiple comparisons test. $n = 4$–6 mice. Reduced recruitment and activation of several subsets of T cells occurred in the skin of MC-deficient mice during DENV infection, which was repaired upon reconstitution of MC-deficient mice with MCs.

compared with Sash mice, but the numbers of activated CD4⁺ T cells were only significantly increased in WT mice 24 hours after infection (Figure 2, H and I). Interestingly, peak γδ T cell activation occurred 3 days after infection (Figure 2E), similar to what was seen in the FP skin (Figure 1G). Experiments using Sash-R mice further confirmed that MCs were sufficient to restore the phenotype of enhanced T cell recruitment and activation that was diminished as a result of MC deficiency (Supplemental Figure 3). With regard to the innate T cells that we assessed, γδ T cells were more abundant in the DLNs during DENV infection, and activation peaked earlier than what we observed in NKT cells, indicating that γδ T cells are probably the first innate T cells to respond to DENV infection.

Validation of MC-dependent T cell recruitment with Mcpt5-Cre/iDTR mice. To further validate our results of MC-dependent T cell recruitment and activation during DENV infection and to rule out any effect that the *c-Kit* mutation might have on the function of other hematopoietic cells, we used a second mouse model, the *Mcpt5*-Cre/iDTR MC ablation model, which is used to assess MC function (24). For this experiment, mice with Cre driven by the

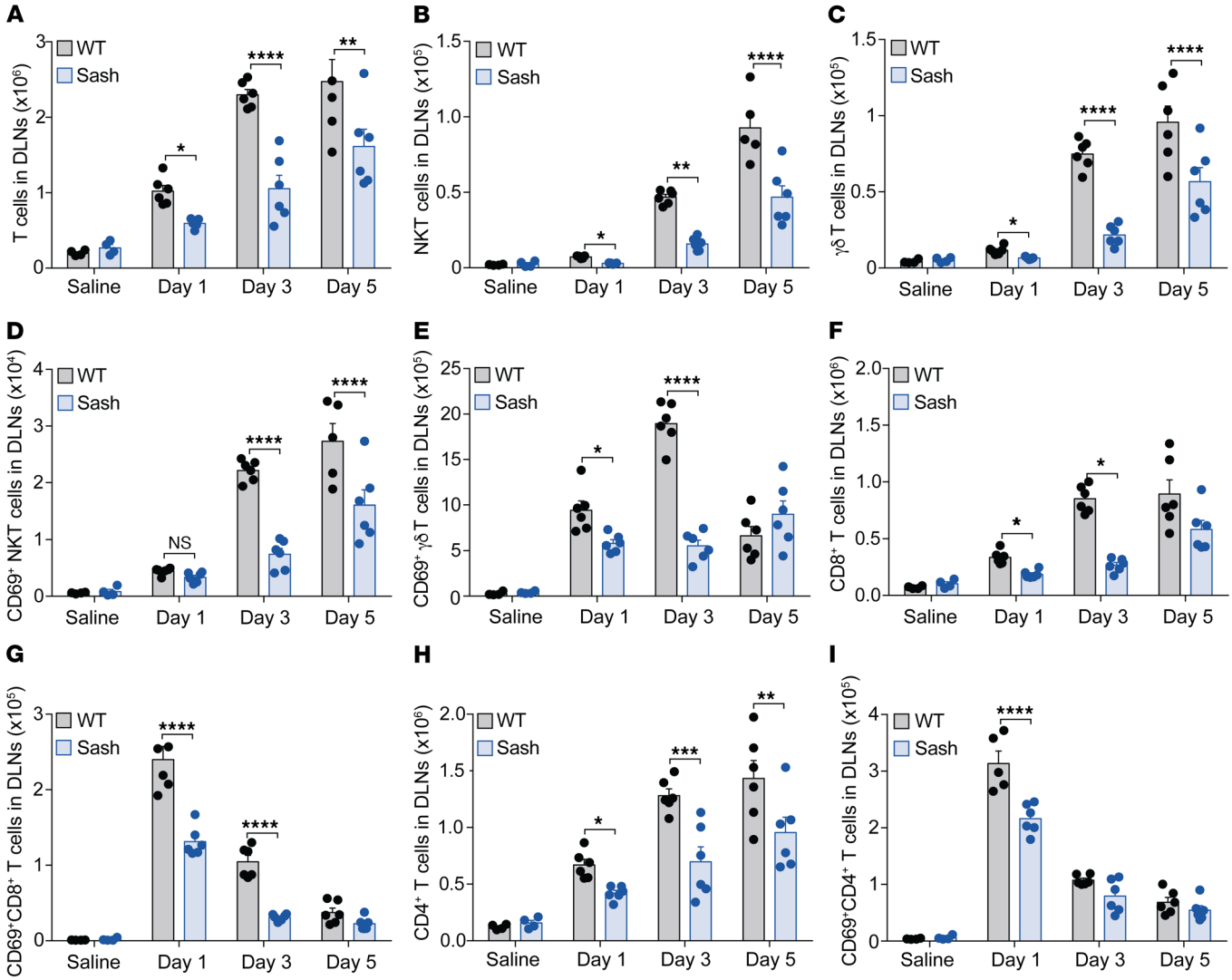

Figure 2. Reduced retention of multiple subsets of T cells in the DLNs and reduced T cell activation in MC-deficient mice. Mice were injected with saline or infected with 1×10^5 pfu DENV via the FP, and popliteal LNs were collected on days 1, 3, and 5 after infection. The LNs were dissociated to make single-cell suspensions, and cells were stained with antibodies against CD45, CD3, CD4, CD8, NK1.1, γδ TCR, and CD69. Numbers of (**A**) total T cells ($CD3^+$), (**B**) NKT cells ($CD3^+NK1.1^+$), (**C**) γδ T cells ($CD3^+\gamma\delta TCR^+$), (**D**) activated NKT cells ($CD3^+NK1.1^+CD69^+$), (**E**) activated γδ T cells ($CD3^+\gamma\delta TCR^+CD69^+$), (**F**) $CD8^+$ T cells ($CD3^+CD8^+$), (**G**) activated $CD8^+$ T cells ($CD3^+CD8^+CD69^+$), (**H**) $CD4^+$ T cells ($CD3^+CD4^+$), and (**I**) activated $CD4^+$ T cells ($CD3^+CD4^+CD69^+$) were compared between WT and Sash mice. Data represent the mean ± SEM. $^*P < 0.05$, $^{**}P < 0.01$, $^{***}P < 0.001$, and $^{****}P < 0.0001$, by 2-way ANOVA with Sidak's multiple comparisons test. n = 4–6 mice per group. MC-deficient mice had defects in recruitment and activation of multiple T cell subsets to DLNs.

MC-specific promoter of *Mcpt5* were crossed with mice bearing an inducible diphtheria toxin receptor (iDTR) to produce mice (*Mcpt5*-Cre/iDTR) that express the DTR only on MCs (24). These mice were injected with diphtheria toxin (DT) at regular intervals using a protocol developed by others (24) to strongly reduce the numbers of peripheral MCs before infecting them with DENV2 (Figure 3A). We validated MC depletion as being greater than 95% (Supplemental Figure 4). Consistent with our data from Sash mice (Figures 1 and 2), in this alternate model of MC deficiency, we observed impaired total T cell retention in the DLNs of MC-depleted *Mcpt5*-Cre/iDTR mice compared with DT-injected *Mcpt5*-Cre congenic controls (Figure 3B). This reduction in T cell retention was consistent for multiple subsets of T cells including NKT cells, γδ T cells, and $CD8^+$ and $CD4^+$ T cells (Figure 3, C–F). Thus, these results using a *c-Kit*–independent, MC-selective ablation model validated our finding that MCs recruit multiple subsets of T cells, including γδ T cells, to the DLNs.

MC-dependent γδ T cell recruitment, proliferation, and activation during infection. Since γδ T cells were the first T cells to respond at the site of infection (Figure 1C) and in DLNs (Figure 2C), we next aimed to determine whether the increase in the numbers of γδ T cells at virus-infected sites was due to proliferation in response to infection or to recruitment directly from the circulation. To distinguish between these 2 cell populations and assess the contributions of MCs to each, we labeled local FP-resident cells by injecting CFSE into the FPs of WT and Sash mice prior to infection with DENV. At the concentration of CFSE used, within 4 hours, we observed that CFSE had labeled approximately 50% of the FP-resident DCs, while less than 1% of the LN cells were labeled (Supplemental Figure 5), indicating that the presence of

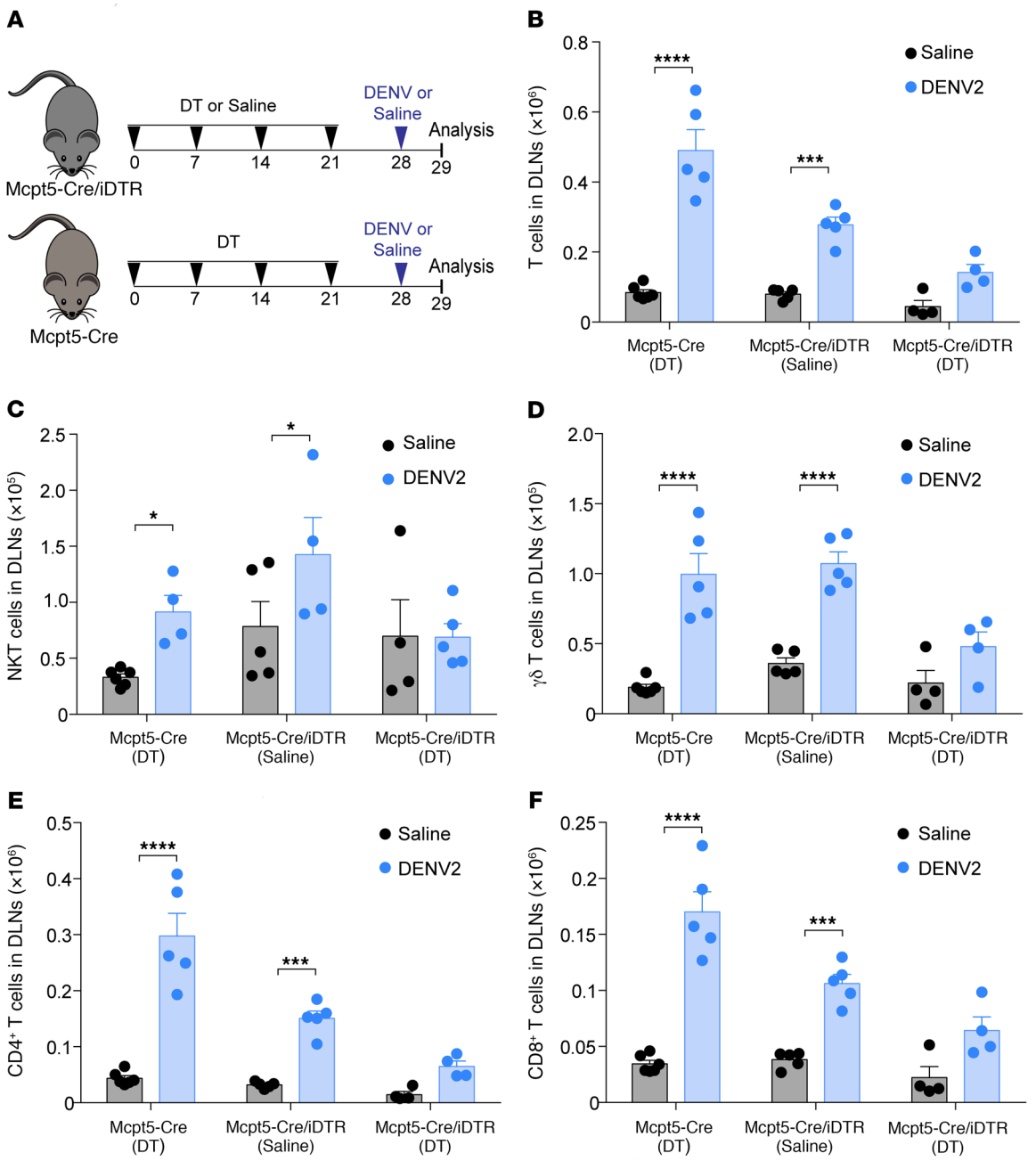

Figure 3. Defects in T cell recruitment to DENV-infected LNs in the MCPT5-Cre iDTR model of MC deficiency. (**A**) Schematic showing the timeline for DT and DENV injections. Mcpt5-Cre and Mcpt5-Cre/iDTR mice were injected with saline to serve as controls or with DT every week for 4 weeks for systemic MC depletion before infection. Mice were injected with saline or infected with 1×10^5 pfu DENV s.c. into the FP, and the popliteal LNs were collected 24 hours after infection. Single-cell suspensions of LN cells were stained to identify T cell subsets using the gating strategy in Supplemental Figure 1. T cell responses to DENV infection were compared among MC-sufficient Mcpt5-Cre/iDTR (saline-injected), MC-sufficient MCPT5-Cre (DT-injected), and MC-deficient Mcpt5-Cre/iDTR (DT-injected) mice. Number of (**B**) total T cells ($CD3^+$), (**C**) NKT cells ($CD3^+NK1.1^+$), (**D**) γδ T cells ($CD3^+\gamma\delta TCR^+$), (**E**) $CD4^+$ T cells ($CD3^+CD4^+$), and (**F**) $CD8^+$ T cells ($CD3^+CD8^+$) all showed MC-dependent recruitment to LNs during DENV infection in this *c-Kit*–independent model of MC deficiency. Data represent the mean ± SEM. $^*P < 0.05$, $^{***}P < 0.001$, and $^{****}P < 0.0001$, by 2-way ANOVA with Sidak's multiple comparisons test. n = 4–6 animals per group. The efficiency of MC depletion after injection with DT is shown in Supplemental Figure 4.

$CFSE^+$ cells in LNs following DENV challenge can be interpreted as showing that they are FP derived. Our results also suggested that local FP-resident γδ T cells underwent proliferation in situ, as evidenced by the increase in total numbers of $CFSE^+$ γδ T cells in the FPs during infection (Figure 4A). In addition to the significant increase in the total number of γδ T cells (Figure 4A), we observed a population of newly recruited or possibly unlabeled proliferating γδ T cells in the FPs in response to infection that were $CFSE^-$ 24 hours after infection (Figure 4A). In MC-deficient Sash mice, both $CFSE^+$ (FP-resident) and $CFSE^-$ cell populations were significantly reduced during infection compared with WT mice (Figure 4A). There was no baseline difference in the levels of resident or

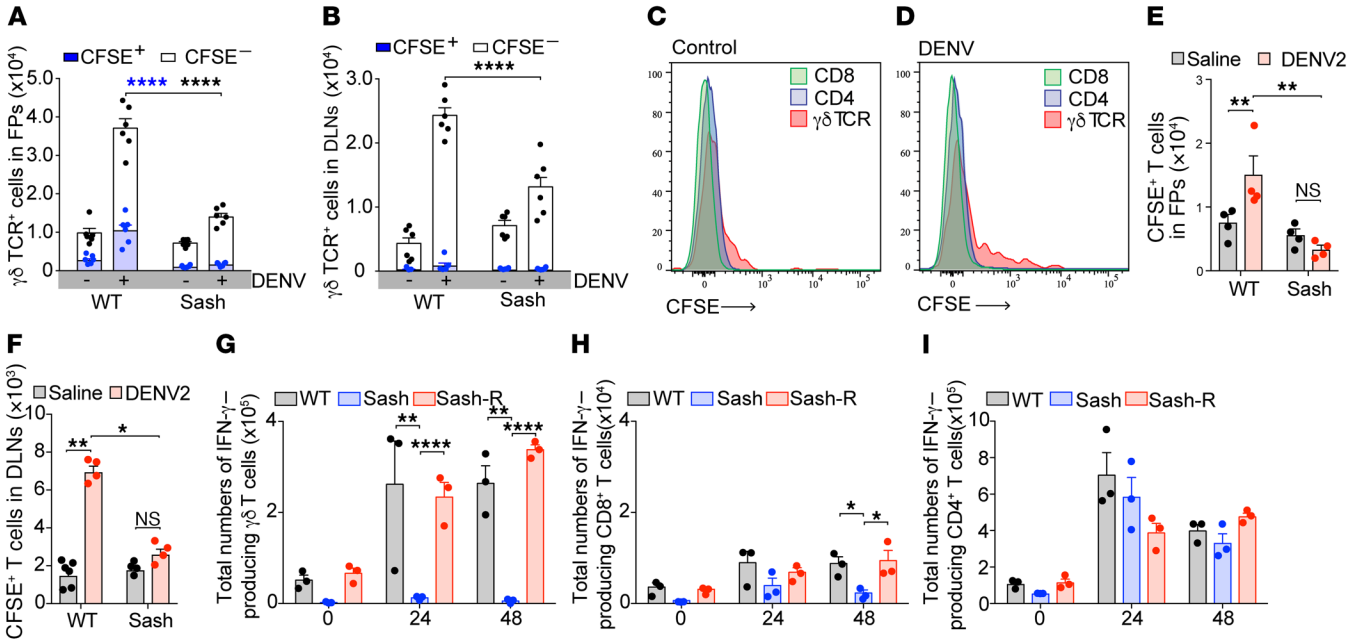

Figure 4. MC-dependent recruitment, proliferation, and activation of γδ T cells at sites of DENV infection. WT and Sash mice were injected with CFSE 4 hours before s.c. FP injection of 1×10^5 pfu DENV or saline. (**A**) FPs and (**B**) DLNs were collected 24 hours after infection, and $CFSE^+$ and $CFSE^-$ γδ T cells were enumerated by flow cytometry. Sash mice showed significantly reduced numbers of both $CFSE^+$ and $CFSE^-$ γδ T cells in FPs compared with WT mice. Representative histograms showing CFSE detection in $CD4^+$, $CD8^+$, and γδ T cell subsets in the DLNs of (**C**) uninfected and (**D**) infected WT mice. γδ T cells but not $CD4^+$ or $CD8^+$ T cells migrated to the DLNs from the site of infection. Multiple peaks in the histogram indicate proliferation of γδ T cells. Recruitment of T cells in the (**E**) FPs and (**F**) DLNs upon infection in WT but not Sash mice was confirmed by injecting CFSE-labeled splenocytes 24 hours prior to infection and analyzing the $CFSE^+$ T cell numbers in FPs and DLNs 24 hours after infection. (**G**–**I**) Single-cell suspensions of LN cells, collected 24 hours and 48 hours after infection, were treated with monensin for 6 hours and then stained for the surface markers CD3, CD4, CD8, and γδ TCR and intracellularly for IFN-γ. Total numbers of IFN-γ–producing cells in WT, Sash, and Sash-R mice were subtyped on the basis of (**G**) γδ, (**H**) $CD8^+$, and (**I**) $CD4^+$ T cells. Data represent the mean ± SEM. $^*P < 0.05$, $^{**}P < 0.01$, and $^{****}P < 0.0001$, by 2-way ANOVA with Sidak's multiple comparisons test. n = 3–6 mice per group.

unlabeled γδ T cells between WT and Sash mice in the uninfected control groups (Figure 4A). We also observed that the numbers of $CFSE^-$ γδ T cells were increased in DLNs following infection of WT mice with DENV (Figure 4B). Similar statistically significant trends in MC-dependent γδ T cell recruitment in response to DENV in FPs and DLNs persisted 72 hours after infection (Supplemental Figure 6). Of note, the FP-derived γδ T cells in the DLNs showed evidence of having proliferated, as determined by dilution of the CFSE stain (Figure 4, C and D, and Supplemental Figure 7).

The increased numbers of $CFSE^-$ γδ T cells were suggestive of recruitment to the LNs; however, given the possibility that the increase in unlabeled γδ T cells could also occur if there were to be substantial proliferation of the unlabeled local cells, we also used an alternative method to confirm that recruitment had occurred. For this, labeled splenocytes were injected into mice prior to DENV infection, and we measured the numbers of $CFSE^+$ T cells and that had trafficked from the circulation into the FP skin (Figure 4E) and DLNs (Figure 4F) by 24 hours after infection. This confirmed that recruitment occurs, in addition to local proliferation, in a MC-dependent fashion. Similarly, we also observed MC-dependent recruitment of the γδ T cell subset in response to DENV in FPs and DLNs (Supplemental Figure 8). These results confirmed that the population of γδ T cells that is augmented by MCs during DENV infection consists of both newly recruited and locally proliferating γδ T cells and that there is significant, MC-dependent recruitment and proliferation of these T cells.

Functional γδ T cell responses rely on induction of IFN-γ in the context of both viral infection and tumor immunosurveillance (18). Thus, to further assess the contributions of MCs to γδ T cell activation in vivo, we quantified the numbers of IFN-γ–producing γδ T cells (Figure 4G) in comparison with the numbers of IFN-γ–producing $CD8^+$ (Figure 4H) and $CD4^+$ (Figure 4I) T cells during DENV infection of WT, Sash, and Sash-R mice. Interestingly, we found that IFN-γ production by γδ T cells at both 24 hours and 48 hours was highly dependent on MCs (Figure 4G). Although $CD8^+$ T cells were not major contributors of IFN-γ, we also detected reduced numbers of $CD8^+IFN\text{-}\gamma^+$ T cells 48 hours after infection in Sash mice compared with WT and Sash-R mice (Figure 4H); however, MCs did not significantly influence the number of $CD4^+IFN\text{-}\gamma^+$ T cells (Figure 4I). These results demonstrate that IFN-γ production by γδ T cells is MC dependent and indicate that γδ T cells are a major cellular source of IFN-γ during DENV infection.

Contact is necessary for MC-dependent γδ T cell activation and proliferation. Having identified MC-dependent γδ T cell activation and proliferation in virus-infected skin, we next questioned whether the influence of MCs on γδ T cells was direct and capable of activating γδ T cells in the absence of other bystander cells in the tissue microenvironment. To begin to address this question, we performed a Transwell assay, in which T cells purified from the LNs of naive mice were applied to the upper compartment of the semiporous chamber, and BMMCs were added to the bot-

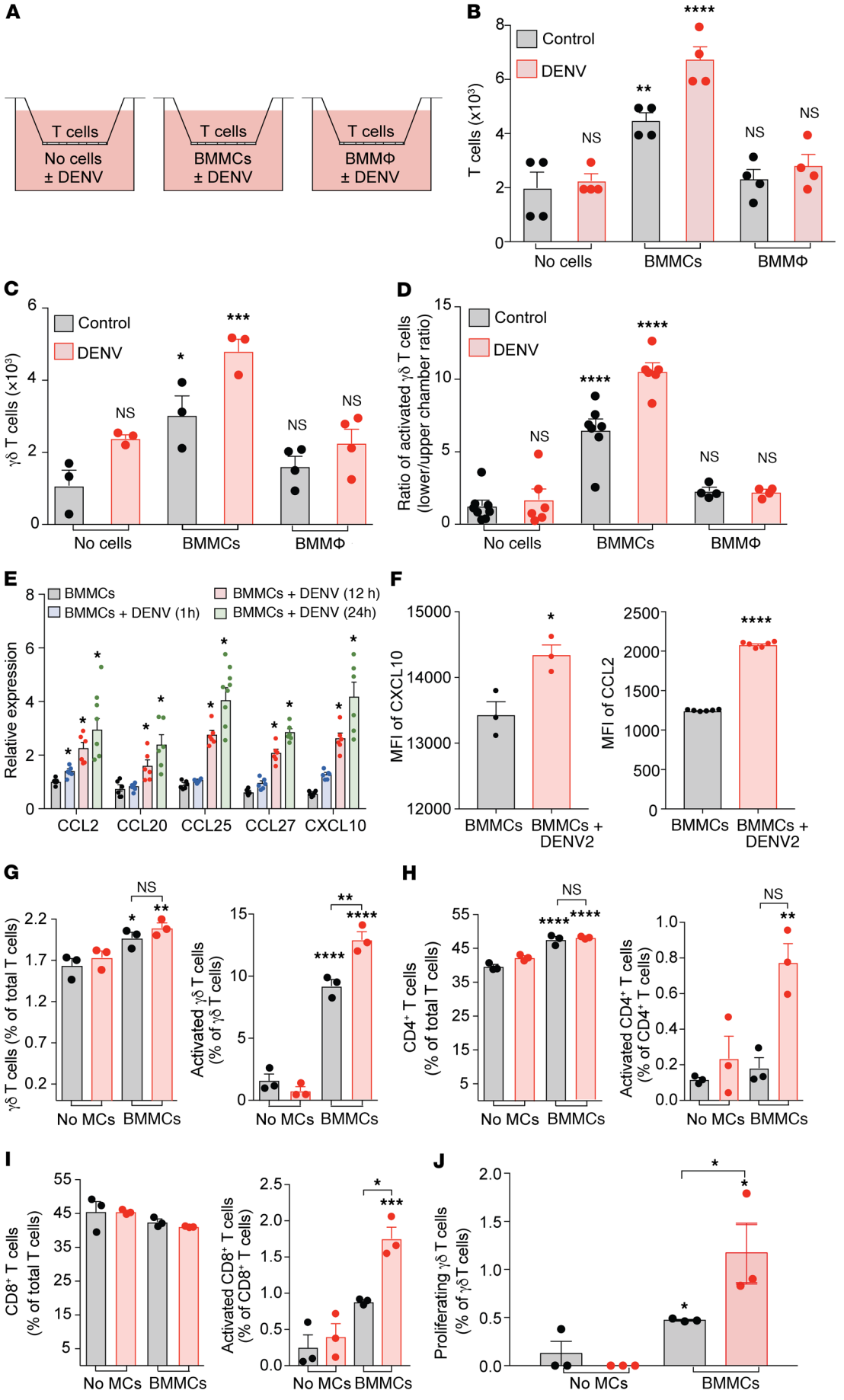
A
T cells
No cells
± DENV
T cells
BMMCs
± DENV
T cells
BMMΦ
± DENV
B
Control
DENV
T cells (x10³)
No cells
BMMCs
BMMΦ
C
Control
DENV
γδ T cells (x10³)
No cells
BMMCs
BMMΦ
D
Control
DENV
Ratio of activated γδ T cells (lower/upper chamber ratio)
No cells
BMMCs
BMMΦ
E
BMMCs
BMMCs + DENV (1h)
BMMCs + DENV (12 h)
BMMCs + DENV (24h)
Relative expression
CCL2
CCL20
CCL25
CCL27
CXCL10
F
MFI of CXCL10
BMMCs
BMMCs + DENV2
MFI of CCL2
BMMCs
BMMCs + DENV2
G
γδ T cells (% of total T cells)
No MCs
BMMCs
Activated γδ T cells (% of γδ T cells)
No MCs
BMMCs
H
CD4⁺ T cells (% of total T cells)
No MCs
BMMCs
Activated CD4⁺ T cells (% of CD4⁺ T cells)
No MCs
BMMCs
I
CD8⁺ T cells (% of total T cells)
No MCs
BMMCs
Activated CD8⁺ T cells (% of CD8⁺ T cells)
No MCs
BMMCs
J
Proliferating γδ T cells (% of γδT cells)
No MCs
BMMCs

Figure 5. MC-dependent recruitment and contact-dependent activation and proliferation of γδ T cells. (**A**) Schematic showing the initial cell locations and conditions for the Transwell assay for **B**–**D**. BMMCs or BMMΦ were infected with DENV in the lower chamber, and T cells (n = 3 mice) were added to the top chamber to analyze migration and activation of T cell subsets across the Transwell. (**B**) Significantly higher numbers of T cells migrated to the bottom chamber containing DENV2-stimulated MCs but not DENV2-infected BMMΦ. (**C**) Among the T cells that migrated to the lower chamber, the γδ T cell subset was enriched in a MC-dependent manner. (**D**) The ratio of activated γδ T cells ($CD3^+\gamma\delta TCR^+CD69^+$) in the lower versus upper chambers showed a significant increase in response to DENV2-stimulated MCs. (**E**) DENV2-stimulated expression of γδ T cell chemoattractants in MCs. (**F**) Intracellular staining for chemokines showed increased CXCL10 and CCL2 production by DENV-treated MCs 24 hours after challenge with DENV, as measured by flow cytometry. (**G**–**I**) Isolated T cells were cultured with BMMCs in the presence or absence of DENV to assess MC-dependent and DENV-dependent activation and proliferation. Cells were stained for CD3, CD4, CD8, CD69, and the γδ TCR and analyzed by flow cytometry after 96 hours of coculture. The percentages of total and activated (**G**) γδ, (**H**) $CD4^+$, and (**I**) $CD8^+$ T cells were compared. (**J**) T cells were labeled with CFSE prior to coculturing with BMMCs, and the percentage of proliferating γδ T cells was measured by flow cytometry. Representative flow cytometric plots are shown in Supplemental Figures 11 and 12. Data represent the mean ± SEM. $^*P < 0.05$, $^{**}P < 0.01$, $^{***}P < 0.001$, and $^{****}P < 0.0001$, by 2-way ANOVA with Tukey's post test (**B**–**E**), Student's unpaired, 2-tailed t test (**F**), and 1-way ANOVA with Tukey's post test (**G**–**J**).

tom chamber, with and without DENV2 as a stimulus (Figure 5A). Although MCs are highly resistant to infection by DENV (5), we included additional controls using bone marrow–derived macrophages (BMMΦ) to determine whether virus-infected cells could also induce responses similar to those of DENV-activated MCs (Figure 5A). Consistent with our in vivo experiments, we observed enhanced migration of total T cells to the bottom chamber when BMMCs were exposed to DENV, indicating that virus-induced MC activation is directly involved in the recruitment of T cells (Figure 5B). In contrast, we observed no enhanced recruitment of T cells by DENV-infected BMMΦ (Figure 5B). Furthermore, the γδ T cell population was preferentially enriched among the T cell subsets that migrated to the lower chamber toward DENV-activated BMMCs (Figure 5C). We found that the ratio of activated γδ T cells in the lower chamber (contact with MCs) relative to the upper chamber (no contact with MCs) was significantly higher when BMMCs were stimulated with DENV, but this was not the case in any of the other control groups (Figure 5D). These data suggest that activation of γδ T cells is both virus dependent and MC dependent, since it occurred only when γδ T cells came in contact with DENV-exposed MCs. However, in contrast, we observed no migration or activation of γδ T cells in response to infected BMMΦ (Figure 5D), highlighting a unique capacity of MCs to recruit and activate γδ T cells.

To identify stimuli that might promote recruitment of γδ T cells by MCs, we measured the expression of known γδ T cell chemoattractants by reverse transcription PCR (RT-PCR). Our results show that CXCL10 was highly induced in MCs upon stimulation with DENV (Figure 5E). We also detected an increase in expression of other chemoattractants that are known to promote T cell migration, including CCL2, CCL20, CCL25, and CCL27 (Figure 5E). We also selected 2 of these chemokines, CCL2 and CXCL10, to confirm that increased cytokine production occurs at the protein level. Using intracellular staining of BMMCs, we observed a significant induction of both CCL2 and CXCL10 expression in DENV-exposed BMMCs (Figure 5F). To further characterize the effects of virus-activated MCs on the stimulation and proliferation of γδ T cells, we performed a coculture experiment, whereby T cells isolated from LNs were incubated with BMMCs in the presence or absence of DENV for 96 hours. Here, MCs promoted the relative expansion of γδ T cells (Figure 5G) and $CD4^+$ T cells (Figure 5H), with no significant influence on the $CD8^+$ T cell population (Figure 5I). Although we have noted some degree of γδ T cell activation in the presence of MCs alone, DENV-specific MC-induced γδ T cell activation was significantly higher (Figure 5G) and began as early as 48 hours after infection (Supplemental Figure 9). This basal increase in MC activation was likely due to soluble factors produced by MCs that were able to act on γδ T cells because of their close proximity in the coculture system. In support of this, we observed that the leukotriene receptor antagonist, but not the TNF-blocking antibody, was able to reduce the basal levels of MC activation in coculture, although the antagonist did not eliminate MC activation completely (Supplemental Figure 10), indicating that multiple factors may be involved. These results show that specific activation of both αβ and γδ T cells can occur by MCs, but, interestingly, γδ T cells showed the highest expansion and percentage activation compared with $CD4^+$ and $CD8^+$ T cells (Figure 5, G–I). Survival of MCs was not influenced over the course of the experiment (data not shown). To validate the MC- and DENV-dependent expansion of γδ T cells, purified cells from naive mice were labeled with CFSE prior to coculture with BMMCs, and the percentage of γδ T cells undergoing proliferation was measured by flow cytometry (Figure 5J). A significant increase in proliferation was apparent when MCs were cocultured with γδ T cells compared with controls, and this proliferation was further increased in the presence of DENV (Figure 5J and Supplemental Figure 11). CFSE dilution occurred in live cells and appeared stepwise on histograms, confirming that the dilution effect was due to proliferation (Supplemental Figure 12). Thus, activation and proliferation of γδ T cells are both MC and DENV dependent.

Immune synapse formation between MCs and γδ T cells in vivo. After establishing the potential of DENV-exposed MCs to activate T cells in vitro, we questioned whether this occurs in vivo. DENV-infected skin was isolated 24 hours after s.c. injection with virus or saline as a control. This tissue was cryosectioned and stained for blood vessels, MCs, and γδ T cells. As MCs are tissue resident and γδ T cells patrol the skin constitutively, we expected to see both cell types in control tissues. Indeed, although γδ T cells were not present in all fields of view (Figure 6A), they could be infrequently located but did not show any clear interactions with MCs (Figure 6B). In contrast, in DENV-infected skin, MC and γδ T cell interactions were widely observed. In some cases, we identified clusters of γδ T cells that appeared very close to activated MCs (Figure 6C). In this case, MC activation was clear because of the presence of extracellular granules near the MCs, suggesting recent degranulation (Figure 6C). These γδ T cells could potentially be at a high density as a result of proliferation in situ or because of recruitment from the proximal blood vessel, since we observed that both proliferation and recruitment occurred in a MC-dependent fashion in the FPs during DENV infection (Figure 4, A and E). Interestingly, we observed physical interactions between

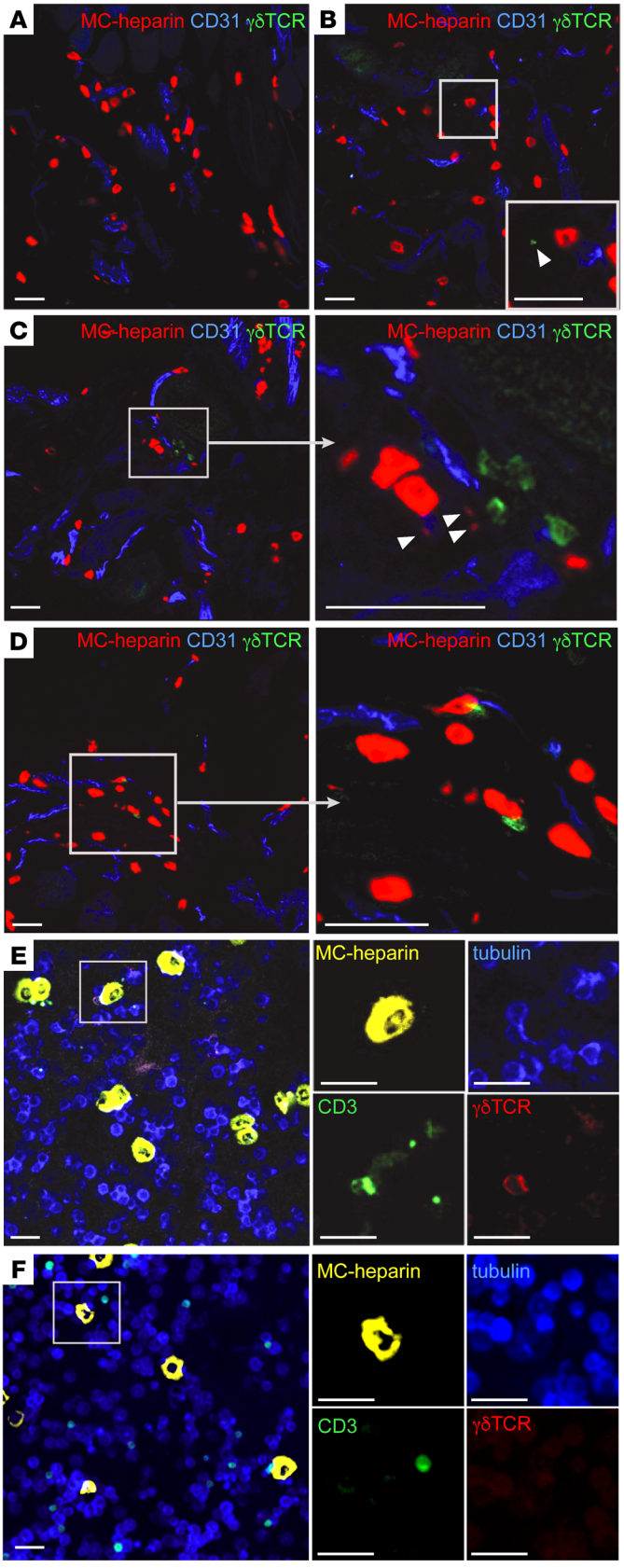

Figure 6. Immunological synapse formation between MCs and γδ T cells at infection sites. Mice (n = 3) were injected with (**A** and **B**) saline or (**C**–**E**) 1×10^5 pfu DENV. FP tissue collected 24 hours after infection was sectioned and stained for blood vessels (CD31, blue) and the γδ TCR (green) and then probed for MC-heparin (MC granules, red). Representative control confocal images in which MCs can be viewed near blood vessels (**A**) without nearby γδ T cells or (**B**) in which γδ T cells appeared infrequently in the same field as MCs. The area in the gray box is enlarged as an inset in **B**, and white a arrowhead indicates γδ T cells. (**C**) In DENV-infected tissues, several γδ T cells clustered around MCs that appeared activated because of MC granules that were extracellular in the tissue (indicated by white arrowheads in the enlarged inset on the right). (**D**) Many γδ T cells formed close contacts with MCs in DENV-infected tissues. Quantification of MC–γδ T cell contacts and additional representative images are provided in Supplemental Figure 13. (**E**) MCs and γδ T cells were observed interacting in the peritoneal cavity 24 hours after i.p. infection with DENV (1×10^6 pfu). Peritoneal lavage cells were cytospun onto glass slides prior to staining with antibodies against CD3, γδ TCR, and tubulin and probing against MC-heparin. MCs and γδ T cells appeared to form stable contacts that were visualized after isolation. Strong polarization of CD3 and γδ TCR toward the MC contact site revealed immune synapse formation. (**F**) No stable contacts between MCs and γδ T cells were observed in cytospins from similarly prepared uninfected peritoneal cells. Additional representative images of MC–γδ T cell conjugates in cytospins from DENV-infected mice and of control cytospins are provided in Supplemental Figure 14. Scale bars: 20 μm; 20 μm (enlarged insets in **B**–**F**).

γδ T cells and MCs, which was supported by the presence of multiple γδ T cell–MC conjugates in the same field of view in a representative image (Figure 6D and Supplemental Figure 13). After quantification across multiple fields of view from multiple animals, we determined that approximately 36% of granulated MCs appeared to physically contact γδ T cells at the skin infection site (Supplemental Figure 13). Likewise, 24 hours after injection of DENV into the peritoneal cavity, we observed conjugates of MCs and γδ T cells (Figure 6E). After cytospinning and staining the peritoneal lavage cells for CD3, γδ TCR, tubulin, and MC-heparin, the nature of the physical interactions could be more clearly discerned. Contact sites between γδ T cells and MCs showed strong polarization and clustering of the γδ TCR and signaling molecule CD3 toward the MC (Figure 6E and Supplemental Figure 14A), while γδ T cells were not identified as interacting with MCs in cytospins from control animals (Figure 6F and Supplemental Figure 14B). Additional representative images from DENV-infected and control skin and from cytospins of peritoneal cells after i.p. infection or saline injection, including those showing multiple γδ T cell–MC conjugates from cells of DENV-infected animals, are provided in Supplemental Figure 14. These images show the extensive recruitment and physical association of MCs and γδ T cells in vivo during DENV infection and, furthermore, suggest antigen presentation by MCs due to the consistent polarization of the γδ TCR during immune synapse formation.

TCR-dependent activation of γδ T cells by MCs. To address the functional consequences of γδ T cells for immune clearance during DENV infection, we examined their ability to kill infected cells. Since DCs are targets of DENV infection in vivo, we used DENV-infected bone marrow–derived DCs (BMDCs) in coculture with total T cells to assess target cell killing. We detected a significant increase in cytotoxicity in DENV2-infected BMDCs that were exposed to total purified T cells, which was lost after deple-

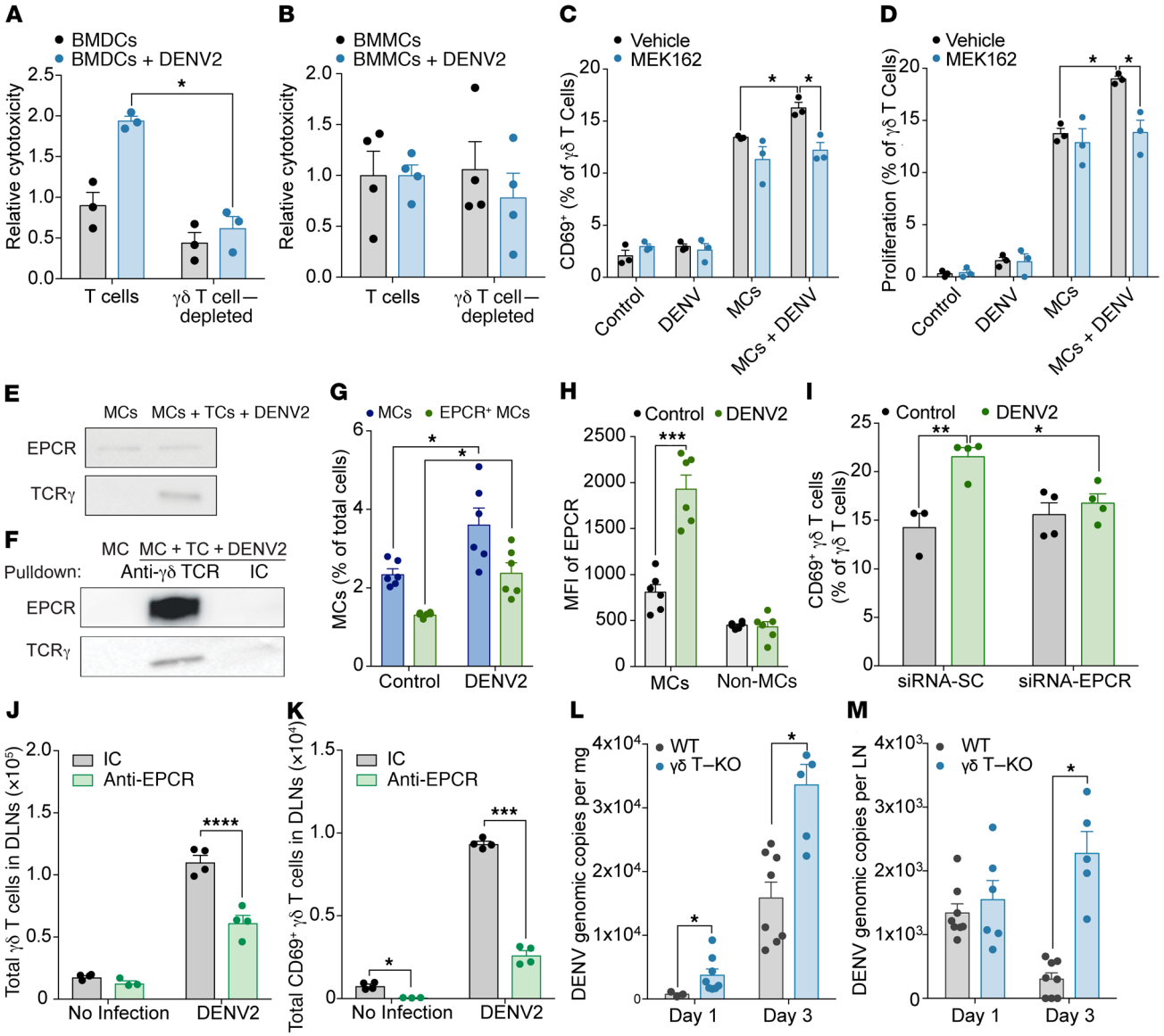

Figure 7. MC- and antigen-dependent γδ T cell activation is mediated through EPCR and γδ TCR, promoting viral clearance. Total T cells or T cells depleted of γδ T cells from DENV-infected LNs, 72 hours after infection, were cocultured with (**A**) BMDCs or (**B**) BMMCs that were preinfected with DENV (MOI = 1). Cytotoxicity was measured by LDH assay and normalized to the control. BMDCs, but not BMMCs, showed cytotoxicity, which was lost with γδ T cell depletion. (**C** and **D**) CFSE-labeled T cells purified from naive mice were cocultured with BMMCs with or without DENV and with or without MEK162. MEK162 inhibited DENV-specific γδ T cell (**C**) activation and (**D**) proliferation, as measured by flow cytometry at 96 hours. (**E**) Lysates from cocultures of DENV-exposed MCs and T cells (TCs) or control MCs were probed for EPCR by Western blotting. γδ TCR was only detected in lysates containing T cells. (**F**) Pulldown of the γδ TCR showed interaction with EPCR, as detected by Western blotting. Pulldown was confirmed by detection of the γTCR subunit. In contrast, pulldown using an isotype control (IC) antibody did not precipitate γδ TCR or EPCR. Increases in (**G**) MCs expressing EPCR and (**H**) expression of EPCR on MCs in LNs was observed 24 hours after infection. Representative flow cytometric plots are provided in Supplemental Figure 16. (**I**) γδ T cells were activated by DENV-exposed MCs transfected with scrambled control siRNA, which was blocked by knockdown of EPCR in MCs. Blocking EPCR in vivo by injection of blocking antibody limited (**J**) accumulation and (**K**) activation of γδ T cells in DLNs following DENV infection. (**L** and **M**) WT and γδ T cell–KO (γδ T–KO) mice were infected with DENV2 via FP injection, and DENV genomic copies were quantified in the FPs and DLNs 24 hours and 72 hours after infection. γδ T cell–KO mice had higher viral loads in the (**L**) FPs and (**M**) DLNs. Data represent the mean ± SEM. $^*P < 0.05$, $^{**}P < 0.01$, $^{***}P < 0.001$, and $^{****}P < 0.0001$, by 2-way ANOVA with Sidak's multiple comparisons test. n = 4–6 mice per group. (See complete unedited blots in the supplemental material.)

tion of γδ T cells from the total T cell pool (Figure 7A), indicating that γδ T cells do indeed kill DENV-infected DCs. The death of the DENV-infected DCs by γδ T cells was also confirmed using an alternate method, in which we measured DC apoptosis by flow cytometry (Supplemental Figure 15). In contrast, BMMCs that were exposed to DENV were not killed (Figure 7B), probably because of their resistance to productive DENV infection (5). These results support the notion that γδ T cells are capable of direct killing of infected target cells but that the interactions between MCs and γδ T cells do not involve target killing.

Given the appearance of immune synapse formation between MCs and γδ T cells (Figure 6E), evidence of γδ T cell activation and

proliferation (Figure 5, D and F), and the confirmation that this interaction does not involve direct killing of MCs (Figure 7B), we strongly suspected that a process similar to antigen presentation by MCs to γδ T cells was occurring and that it involved activation of γδ TCR. To determine whether MCs activate γδ T cells through the TCR, we used the specific inhibitor of the MEK/ERK pathway, MEK162, which is required for TCR signaling (25, 26). T cells were cultured with and without MCs and DENV, after which the activation (Figure 7C) and proliferation (Figure 7D) of the γδ T cell subset were measured. We found that MCs alone induced the activation and proliferation of γδ T cells, which was further increased by DENV (Figure 7, C and D). Inhibition of TCR signaling blocked the MC- and DENV-dependent activation and proliferation of γδ T cells, but not the MC-dependent and DENV-independent activation (Figure 7, C and D). This indicates that MCs activate γδ T cells and induce their proliferation, which occurs mechanistically through the γδ TCR in the presence of virus.

To identify the mechanism of γδ T cell activation by MCs, we cocultured MCs with T cells and pulled down the γδ TCR using a monoclonal antibody. By Western blotting, we observed TCRγ in whole-cell lysates from T cell and MC cocultures (Figure 7E). EPCR could also be specifically detected in the lysate fractions (Figure 7E). Western blot analysis on the fractions after γδ TCR pulldown confirmed pulldown of the TCRγ subunit and also revealed that EPCR was a protein associated with the γδ TCR (Figure 7F). Use of an isotype control antibody for pulldown confirmed the specificity of this interaction (Figure 7F). EPCR is a transmembrane glycoprotein and nonconventional antigen presentation molecule closely related to CD1d that has previously been described to interact with γδ TCR (27). To validate that EPCR is expressed on MCs in vivo, we performed flow cytometric analysis on uninfected and DENV-infected DLNs. Indeed, we found that MCs expressed EPCR and that there was a significant increase in the number of EPCR$^+$ MCs in DLNs during DENV infection (Figure 7G and Supplemental Figure 16A). EPCR expression on MCs was also increased (Figure 7H and Supplemental Figure 16, A and B), whereas the number of EPCR$^+$ non-MCs and levels of EPCR on non-MCs were not significantly changed (Figure 7H and Supplemental Figure 16, C and D). To determine whether EPCR expression on MCs functionally affects γδ T cell activation during DENV infection, we also used a siRNA against *EPCR* (siRNA-EPCR) to determine whether it could block MC-mediated DENV activation of γδ T cells, compared with scrambled control siRNA (siRNA-SC). We detected no increase in cell activation in γδ T cells cocultured with BMMCs transfected with siRNA-EPCR (which showed ~83% knockdown) (Supplemental Figure 17), while siRNA-SC transfection of BMMCs did not inhibit γδ T cell activation resulting from the coculture (Figure 7I). To confirm that EPCR is required for γδ T cell activation in vivo, we performed an experiment in which a blocking and neutralizing antibody against EPCR was injected into FPs prior to infection with DENV. In support of the critical role of EPCR in γδ T cell activation during DENV infection, the numbers of both total (Figure 7J) and activated (Figure 7K) γδ T cells were reduced in the DLNs of animals that had been administered the EPCR-blocking antibody. These results show that EPCR is a critical component of the immune synapse between MCs and γδ T cells during DENV infection and that it promotes γδ T cell activation and proliferation.

Finally, to validate the importance of γδ T cells in the clearance of DENV infection in vivo, we infected γδ T cell–deficient (γδ T cell–KO) mice (28) with DENV and monitored the infection levels in the skin of the FP, the site of infection (Figure 7L), and the LNs (Figure 7M). Quantification of DENV by real time RT-PCR showed that the viral burden was much higher in γδ T cell–KO mouse FPs 24 hours after infection than in the FPs of WT control mice (Figure 7L). By 72 hours after infection, viral titers were higher in the γδ T cell–KO mice in both the FP and LNs (Figure 7, L and M). These results confirm that γδ T cells contribute to clearance of DENV in vivo.

Discussion

Although they are both responsible for surveillance at the front line of immune defense, MCs and γδ T cells have not to our knowledge been reported to interact with each other. This study demonstrates that antigen presentation by MCs to γδ T cells promotes γδ T cell activation through a TCR-dependent mechanism. Our findings show that, in turn, γδ T cells promote the early and direct killing of virus-infected cells, as shown by the fact that γδ T cell–deficient animals have highly impaired clearance of virus from the site of infection and DLNs.

At the initiation of inflammation to DENV in the skin, we observed MC-dependent recruitment of several subsets of T cells to the site of infection. This is consistent with previous studies that demonstrated the MC-dependent recruitment of NKT cells and CD8$^+$ T cells to sites of viral infection (5). However, prior studies did not definitively ascribe the role of viral clearance to recruited T cells or reveal further mechanisms related to how the newly recruited cells could promote immunity. Taking a systematic approach to describe the subsets of T cells recruited to the DENV-infected skin, we demonstrated that γδ T cells were the earliest responding T cell subset and that their recruitment was also MC dependent. Since γδ T cells are known to patrol the skin, we expected that their increased numbers in the tissue might only be due to local proliferation. Our results using CFSE labeling of local tissue-resident cells showed that this is only a partial explanation for the enrichment of γδ T cells in DENV-infected skin, since there was a substantial increase in the nonlabeled portion of γδ T cells, which was suggestive of recruitment. However, a caveat to this interpretation is our observation that CFSE labeling in the tissue was not 100%, and it is likely that, in addition to recruitment, proliferation of unlabeled cells could explain a portion of the increase in unlabeled cells. Adoptive transfer of CFSE-labeled T cells to recipients prior to cutaneous DENV infection confirmed the recruitment of blood-derived T cells, including those of the γδ subset, into the skin. Although it is important to acknowledge that CFSE-labeling experiments have caveats (29), these labeling experiments in MC-deficient mice support the idea that MCs induce both the recruitment and local proliferation of responding γδ T cells.

We observed that γδ$^+$ T cells, CD8$^+$ T cells, and NKT cells were all recruited in a MC-dependent fashion to the infected skin, while CD4$^+$ T cells were not substantially increased at early time points. This is probably because most CD4$^+$ T cells in the skin are Tregs, which would not be beneficial to the clearance of virus. In contrast, CD4$^+$ T cells are recruited abundantly in the DLNs during

DENV infection, but most of those cells are traditional αβ Th cells. The influx of LN T cells is most likely the result of LN hypertrophy, which is dependent on MC-derived TNF (10). Further studies will be needed to define how MC contributions to LN hypertrophy shape downstream functions of $CD4^+$ T cells.

There are multiple indications in our data that MCs are more consequential to T cell recruitment than are infected cells. First, we observed in Sash mice that there were higher levels of infection in the skin, but in spite of this, there was greatly reduced recruitment of T cells at early time points. Second, even in Transwell experiments in which infection-permissive cells were used, T cell chemotaxis did not occur as significantly as it did when MCs were activated on the opposite side of the Transwell. Despite not showing direct chemotaxis toward infected MΦ, T cells were clearly still able to identify and kill infected cells, since cytotoxicity levels increased in infected DCs compared with levels in uninfected DCs in direct coculture. MCs, in contrast, are not significant targets for T cell killing, probably because they are very resistant to DENV infection (5). In spite of this, our previous study suggested that features of MC activation were consistent with the process of abortive replication, since they apparently internalized virus particles, and activation of MCs and cytokine production in response to DENV were dependent on cytosolic pattern recognition molecules such as TLR3 and MDA5 (5). These observations point to the conclusion that MCs act as immunosurveillance cells, promoting the recruitment and activation of T cells so that nearby infected cells can be targeted for killing.

Whether MCs are nonclassical APCs has been debated. Some mechanisms through which MCs could contribute indirectly to antigen presentation have been postulated and include, for example, the passing of antigen to DCs for further processing and presentation (30) or the release of exosomes that might come in contact with T cells and induce their activation (31). Multiple studies have shown that MCs and T cells can physically interact in tissues (16), and we previously observed that MCs interact with $CD3^+$ cells in DENV-infected skin (5), but it has not been clear if this interaction occurs as a component of the normal surveillance role of T cells in tissues (11). Several of our results presented here indicate that the interaction between MCs and γδ T cells is more analogous to "professional" antigen presentation rather than endogenous or "nonprofessional" antigen presentation. First, we observed that MCs and γδ T cells form conjugates in vivo that are characterized by polarization of the γδ TCR toward the MC contact site. This indicates that immune synapses form, even though MCs themselves are not targets of killing. Second, we observed that a significant portion of the γδ T cell activation and proliferation occurs only in the presence of DENV. Third, T cell activation was dependent on TCR signaling cascades. This was shown by the observation that the ERK pathway inhibitor, which was used to block TCR activation, completely abrogated the antigen-dependent component of γδ T cell activation. Like other groups (11), we also saw a certain amount of nonspecific γδ T cell activation that was MC contact dependent. While there was a baseline increase in T cell activation upon coculture with MCs, this was likely due to secretion of soluble factors including leukotrienes, since a portion of the response was inhibited by the leukotriene receptor antagonist montelukast. Other studies also showed that soluble factors, including TNF, that are released by MCs can contribute to increased basal T cell activation (32), although in our coculture, TNF blockade did not affect the basal activation levels. It should also be noted that we observed antigen-specific activation of traditional αβ $CD4^+$ and $CD8^+$ T cells, which is also suggestive of traditional antigen presentation by MCs and warrants future exploration of the functional consequences for immunity. Here, we focused on identifying the mechanism of TCR-dependent activation of γδ T cells by MCs. Pulldown of the γδ TCR revealed that it is physically associated with the nonclassical antigen presentation molecule EPCR. Other studies have also shown that EPCR is a ligand for the γδ TCR, which suggested it could be a ligand for infected or stressed cells (27). Interestingly, the EPCR molecule binds the phospholipid phosphatidylethanolamine (33), which is present on DENV particles and is probably derived from the ER membrane used for virus budding (34). Blocking of EPCR in MCs, either with a siRNA or a neutralizing antibody, was also shown to significantly prevent γδ T cell activation both in vitro and in vivo. Our data suggest that the interaction of these molecules is critical for γδ T cell activation, but there may be other important molecules that participate in the interaction between MCs and γδ T cells.

Although γδ T cells have been shown in some cases to bind to viral glycoproteins, resulting in direct activation, independent of antigen presentation, we observed that DENV alone had minimal influence on γδ T cells and did not result in significant levels of activation. Our results also indicated that $CD4^+$ T cells, though not significantly recruited by MCs to sites of DENV infection, expanded in coculture in the presence of MCs. This suggests that MCs are also able to activate $CD4^+$ cells in an antigen-dependent manner, but it is not clear from these data whether this would occur in vivo, since there are very few MCs in DLNs where $CD4^+$ T cells are abundant, and those in the DLNs are primarily confined to the LN sinuses (35, 36), segregated away from T cell zones. Future studies are needed to understand the molecules that are used by MCs to present antigen to conventional T cells.

Activation of γδ T cells by MCs involves upregulation of the activation marker CD69 and proliferation, which was shown to be MC dependent. Consistent with these findings, IFN-γ production, another indicator of γδ T cell activation, was absent in Sash mice in the γδ T cell subset. It is also interesting to note, in the context of DENV immune defense, that γδ T cells were the primary T cell subset that produced IFN-γ at early time points of infection. Using γδ T cell–KO mice, we also confirmed that the MC-initiated and -dependent recruitment of γδ T cells is physiologically relevant during peripheral viral infection, since γδ T cell–KO animals had higher viral titers at the site of infection and in secondary target organs. This is consistent with findings of prior studies showing that γδ T cells are important for clearance of West Nile virus (19, 20), which is closely related to DENV. Interestingly, since the DENV replication cycle requires approximately 12 hours for completion, our evidence that γδ T cells promote lower virus titers within 24 hours of infection emphasizes that these cells are capable of responding to infection and killing target cells that have been infected within the first or second amplification cycles of the virus in vivo. This contrasts with the role of MCs we observed pre-

viously during systemic infection, in which widespread activation of MCs was found to contribute significantly to inducing vascular leakage and pathological signs of DENV disease (37). Prior to systemic infection, early MC activation is protective, having the potential to significantly limit the infection burden in vivo through the recruitment and activation of T cells. Taken together, we believe our results define a new role for MCs as nonconventional APCs in peripheral tissues that are responsible for the recruitment and TCR-mediated activation of γδ T cells, leading to viral infection clearance.

Methods

Animal studies. All animal experiments were conducted in the vivarium at Duke-NUS Medical School. C57BL/6 mice were purchased from InVivos. MC-deficient Sash mice (W^{sh}/W^{sh}) and γδ T cell–deficient mice (B6.129P2-*Tcrd*^{tm1Mom}/J) were originally purchased from The Jackson Laboratory and bred in-house. Mcpt5-Cre/iDTR mice were generated by crossing Mcpt5-Cre mice (provided by Axel Roers, Dresden University, Dresden, Germany) with a Cre excision reporter strain, iDTR (C57BL/6-*Gt(ROSA)26Sor*$^{tm1(HBEGF)Awai}$/J), from The Jackson Laboratory. For all strains, 6- to 8-week-old female mice were used for the experiments.

Infections. For infections, Eden2, a clinical isolate of DENV2, was used. This low-passage clinical isolate was originally obtained from the Duke-NUS reference laboratory and derived from the Early Dengue Infection and Outcome (EDEN) clinical study (38). Viral strains were propagated in *Aedes albopictus* C6/36 mosquito cells (CRL-1660, ATCC), maintained in RPMI medium 1640 with 25 mM HEPES, and titered using standard methods (5, 39). Mice were infected with 1×10^5 pfu DENV s.c. into the FPs or by i.p. injection of 1×10^6 pfu DENV. Sash mice were i.v. injected with 1×10^7 mature BMMCs from congenic controls to generate Sash-R mice as previously described (5). Mcpt5-Cre/iDTR mice were injected with DT (25 ng/g BW) every week for 4 weeks for systemic MC depletion before infection, following a previously published protocol (24). Depletion efficiency was assessed by flow cytometry. For in vivo labeling of T cells, 1×10^{-6} mmol CellTrace CFSE (Thermo Fisher Scientific) was injected s.c. into the FPs of mice 4 hours prior to infection with DENV, according to an established protocol (9). To verify the migration of blood-derived cells into the FPs and LNs, splenocytes from mice were labeled ex vivo with CellTrace CFSE at a final concentration of 5 μM after lysis of RBC. CFSE-labeled splenocytes (1×10^7) were then adoptively transferred into recipient mice by tail-vein injection. In vivo blocking of EPCR (Thermo Fisher Scientific, 16-2012-83) was achieved by s.c. injection of 5 μg monoclonal antibody 24 hours and 4 hours prior to infection. For controls, an IgG isotype control (Thermo Fisher Scientific, 16-4031-81) was similarly injected prior to infection.

Flow cytometry. FP skin and popliteal LNs were harvested and dissociated with collagenase (MilliporeSigma) before passing through a cell strainer (BD Biosciences) to make single-cell suspensions. Total cell numbers were determined by counting with a hemocytometer. Cells were then stained with anti–CD45-BUV395 (564279), anti–CD3e-PercP-Cy5.5 (551163), anti–CD4-BV650 (563232), anti–CD8a–Alexa 700 (557959), anti–CD69-FITC (557392), and anti–CD25-BV785 (564023) (all from BD Biosciences); anti–NK1.1-PE (eBioscience, 12-5941-82); and anti–γδ TCR–APC (BioLegend, 118116). Depletion of MCs in skin and peritoneum was confirmed by staining the cells from FPs and peritoneal lavage with anti–CD45-BUV395, anti–c-Kit–APC (both from eBioscience, 17-1171-82), and anti–FcεR1α-PE (Invitrogen, Thermo Fisher Scientific, 12-5898-82). Expression of EPCR on MCs in LNs was measured by staining cells with anti–c-Kit–PE-CY7 (catalog 105814), anti–FcεR1α-PE (catalog 134308), and anti–EPCR-APC (catalog 141506) antibodies (all from BioLegend). For intracellular IFN-γ staining (using anti–IFN-γ–BV711, BD Biosciences, 564336), cells were first incubated with 2 μM monensin (BioLegend) for 6 hours at 37°C. Intracellular staining for CXCL10 (catalog 701225) and CCL2 (catalog 12-7096-81) was performed by similar methods in BMMCs using antibodies from Thermo Fisher Scientific. Flow cytometric data were acquired with a LSRFortessa cell analyzer (BD Biosciences) and analyzed using FlowJo software.

Virus quantification. DENV genomic copy numbers in the FPs and LNs were quantified by homogenizing tissues in tissue lysis buffer (QIAGEN, Buffer RLT) with ceramic beads (Glen Mills) using a mechanical homogenizer (QIAGEN). Total RNA was isolated using the RNeasy Kit (QIAGEN) according to the manufacturer's protocol. cDNA was synthesized using the iScript cDNA Synthesis Kit (Bio-Rad), with 5 pmol DENV2 primer added to the reaction mix. DENV2 forward and DENV2 reverse primers (Supplemental Table 1) were used for quantification with SYBR Green Reagent (Bio-Rad) in a CFX96 Touch Real-Time PCR Detection System (Bio-Rad). Copy numbers were then calculated using a DENV standard curve generated from serial dilutions of a DNA plasmid containing the DENV genomic sequence.

Transwell and coculture assays. To generate BMMCs, bone marrow was flushed from naive C57BL/6 mouse femurs and cultured in RPMI medium containing 10% FBS, 1% supernatant from Cho-KL cells, which contains stem cell factor (produced in-house), penicillin and streptomycin, HEPES, trypsin inhibitor, sodium pyruvate (Thermo Fisher Scientific), and recombinant IL-3 (5 ng/ml, R&D Systems). After 4 weeks, MCs were verified to be more than 95% pure by toluidine blue staining (MilliporeSigma) prior to use. BMMΦ were prepared as described elsewhere (40). T cells from LNs of naive C57BL/6 mice were purified using a Pan T Cell Isolation Kit II for mouse (Miltenyi Biotec), according to the manufacturer's instructions. For Transwell migration assays, 1×10^5 T cells were applied to Transwell inserts with 3-μm pores (BD Biosciences), and 1×10^5 BMMCs or BMMΦ were grown in the lower chamber in a 24-well plate. Cells were infected using a MOI of 1 of DENV2 for 1 hour in the lower chamber prior to placing the inserts and adding T cells to the top chamber of the Transwell. T cell numbers in the upper chamber were counted after 12 hours and subtracted from the initial count to determine the number of T cells that migrated to the bottom chamber. Flow cytometry was used to characterize the subsets of T cells that migrated to the bottom chamber.

For coculture assays, 1×10^5 BMMCs were mixed with 1×10^5 T cells in complete RPMI with 20 U/ml mouse IL-2 (MilliporeSigma) for 48 to 96 hours. To challenge BMMCs with DENV2, BMMCs were incubated with DENV (MOI = 1) for 1 hour prior to coculturing. Flow cytometry was performed to characterize the frequency of T cells after coculturing. MEK162 (Selleckchem) was used at a concentration of 0.2 μM for the inhibition assay.

For siRNA-mediated knockdown of BMMCs, BMMCs were transfected with 200 nM EPCR siRNA or scrambled control (Santa Cruz Biotechnology) using 4D-Nucleofector (Lonza). Knockdown efficiency was checked 24 hours after transfection using the primers provided by

Santa Cruz Biotechnology in the siRNA kit. These cells were then cocultured with T cells for 72 hours before measuring the effect of EPCR knockdown on γδ T cell activation.

Cytotoxicity and proliferation assays. A lactate dehydrogenase (LDH) cytotoxicity assay (Thermo Fisher Scientific) was used according to the manufacturer's instructions to assess the ability of γδ T cells to lyse DENV-infected DCs. To assess the cytotoxic ability of activated γδ T cells ex vivo, T cells were isolated from the LNs of DENV2-infected mice 72 hours after infection using the Miltenyi Pan T Cell Isolation Kit II for mouse (Miltenyi Biotec). γδ T cells were then depleted from total T cells using a TCR γδ$^+$ T Cell Isolation Kit for mouse (Miltenyi Biotec). The cytotoxic ability of γδ T cells was inferred by comparing the cytotoxic activity of total T cells and γδ-depleted T cells. BMDCs were prepared as described previously (41). BMMCs and BMDCs were exposed to DENV2 (MOI = 2) for 24 hours prior to coculture with T cells or γδ-depleted T cells to measure cytotoxicity. In addition to the LDH assay, BMDCs treated in the aforementioned way were also stained with annexin V–FITC and propidium iodide (PI) 24 hours after coculture, and cytotoxicity was measured by determining the percentage of annexin V$^+$ and PI$^+$ BMDCs. For the measurement of T cell proliferation, T cells were first labeled with CellTrace CFSE (Thermo Fisher Scientific) according to the manufacturer's instructions, prior to coculturing with BMMCs, with and without DENV2 (MOI = 1). Viability was assayed using a LIVE/DEAD Fixable Near-IR Dead Cell Staining Kit (Thermo Fisher Scientific) according to the manufacturer's instructions. Proliferation was measured by dilution of CFSE in live γδ T cells using flow cytometry.

Chemokine expression analysis. BMMCs were challenged with DENV2 (MOI = 1), and cells were harvested after 3, 6, 12, and 24 hours. Total RNA was isolated using the RNeasy Kit (QIAGEN) according to the manufacturer's instructions. Expression of chemokines (*CCL2*, *CCL20*, *CCL25*, *CCL27*, and *CXCL10*) was then determined using the primers listed in Supplemental Table 1. Relative expression was calculated by normalization to the expression of GAPDH and actin using Bio-Rad CFX 3.1 software.

Immunofluorescence microscopy. FPs were frozen in OCT compound (Tissue Tek) and then sectioned (10-μm thickness) using a cryostat (Leica). Sections were acetone fixed at 4°C and then blocked with PBS containing 1% BSA prior to staining with the following primary antibodies: anti-CD31 (BD Biosciences); anti–γδ TCR (BioLegend, 118101); and avidin-TRITC (Thermo Fisher Scientific). The secondary antibodies used were: anti–rat Dy405 (Abcam, ab175671) and anti-hamster-AF647 (Thermo Fisher Scientific, A21451). For staining of peritoneal cells, cells were first cytospun onto glass slides before fixation with acetone. The primary antibodies used were: anti–CD3-FITC (Thermo Fisher Scientific, HM3501); anti–γδ TCR–APC (BioLegend, 118116); anti-tubulin (Thermo Fisher Scientific, MA1-80017); and avidin-TRITC (Thermo Fisher Scientific). The secondary antibody used for tubulin staining was anti–mouse AF405 (Abcam, ab175658). Slides were mounted with Prolong Gold Antifade Reagent (Thermo-Fisher Scientific), and images were acquired using a Carl Zeiss LSM710 confocal microscope. Images show single optical sections acquired in channel series. Merged images contain all channels, and colocalization images were generated using ImageJ software (NIH).

Immunoprecipitation assays. Total T cells isolated from naive mice were depleted of CD4$^+$ and CD8$^+$ T cells using microbeads (Miltenyi Biotec). The remaining T cells were then cocultured with BMMCs exposed to DENV2 (MOI = 1) for 1 hour at a 1:5 ratio. Cells were pelleted after 24 hours and washed twice with cold PBS. Cells were then lysed in RIPA buffer with 1× protease inhibitor cocktail. Cell lysates precleared with Protein A/G Agarose Beads (Thermo Fisher Scientific) were then incubated overnight with 2 μg anti–γδ TCR antibody (BioLegend, 118101) or isotype antibody (BioLegend, 400901) in the cold room, followed by incubation with protein A/G agarose beads for 6 hours. The beads were washed 3 times with lysis buffer, and protein complexes were fractioned by SDS-PAGE. Proteins were detected on Western blots with polyclonal anti–γ TCR (Santa Cruz Biotechnology, SC-25609) and anti-EPCR (Thermo Fisher Scientific, PA5-32217) antibodies.

Statistics. To determine statistical significance, unpaired 2-tailed Student's *t* tests or 1-way or 2-way ANOVA were performed as appropriate using Excel (Microsoft) or GraphPad Prism (GraphPad Software). A *P* value of 0.05 or less was considered significant. Error bars represent the SEM.

Study approval. All animal experiments were performed according to protocols approved by the IACUC of SingHealth (Singapore).

Author contributions

Experiments were primarily performed by CKM. Both authors contributed to experimental design, data analysis, and interpretation. ALS conceived the study and wrote the manuscript. CKM reviewed the manuscript and contributed to its revision.

Acknowledgments

We thank Abhay Rathore (Duke University Medical Center) for discussions and critical manuscript review and Axel Roers (Dresden University, Dresden, Germany) for permission to use the MCPT5-Cre mice for this study. This work was funded by the National Medical Research Council (NMRC) of Singapore (grant no. NMRC/CBRG/0084/2015) and by start-up funding from Duke-NUS Medical School.

Address correspondence to: Ashley St. John, Program in Emerging Infectious Diseases, Duke-National University of Singapore Medical School, 8 College Road, Level 9, 169857, Singapore. Phone: 65.9771.7231; Email: ashley.st.john@duke-nus.edu.sg.

1. Abraham SN, St John AL. Mast cell-orchestrated immunity to pathogens. *Nat Rev Immunol*. 2010;10(6):440–452.
2. Galli SJ, Nakae S, Tsai M. Mast cells in the development of adaptive immune responses. *Nat Immunol*. 2005;6(2):135–142.
3. Tsai M, Grimbaldeston M, Galli SJ. Mast cells and immunoregulation/immunomodulation. *Adv Exp Med Biol*. 2011;716:186–211.
4. St John AL, Abraham SN. Innate immunity and its regulation by mast cells. *J Immunol*. 2013;190(9):4458–4463.
5. St John AL, et al. Immune surveillance by mast cells during dengue infection promotes natural killer (NK) and NKT-cell recruitment and viral clearance. *Proc Natl Acad Sci U S A*. 2011;108(22):9190–9195.
6. Orinska Z, Bulanova E, Budagian V, Metz M, Maurer M, Bulfone-Paus S. TLR3-induced activation of mast cells modulates CD8+ T-cell recruitment. *Blood*. 2005;106(3):978–987.
7. Ebert S, et al. Mast cells expedite control of pulmonary murine cytomegalovirus infection by enhancing the recruitment of protective CD8 T cells to the lungs. *PLoS Pathog*. 2014;10(4):e1004100.
8. Kunder CA, St John AL, Abraham SN. Mast cell

modulation of the vascular and lymphatic endothelium. *Blood*. 2011;118(20):5383–5393.
9. Shelburne CP, et al. Mast cells augment adaptive immunity by orchestrating dendritic cell trafficking through infected tissues. *Cell Host Microbe*. 2009;6(4):331–342.
10. McLachlan JB, et al. Mast cell-derived tumor necrosis factor induces hypertrophy of draining lymph nodes during infection. *Nat Immunol*. 2003;4(12):1199–1205.
11. Kambayashi T, Laufer TM. Atypical MHC class II-expressing antigen-presenting cells: can anything replace a dendritic cell? *Nat Rev Immunol*. 2014;14(11):719–730.
12. Nakae S, et al. Mast cells enhance T cell activation: importance of mast cell costimulatory molecules and secreted TNF. *J Immunol*. 2006;176(4):2238–2248.
13. Mor A, Shefler I, Salamon P, Kloog Y, Mekori YA. Characterization of ERK activation in human mast cells stimulated by contact with T cells. *Inflammation*. 2010;33(2):119–125.
14. Frandji P, et al. Antigen-dependent stimulation by bone marrow-derived mast cells of MHC class II-restricted T cell hybridoma. *J Immunol*. 1993;151(11):6318–6328.
15. Hong GU, Kim NG, Kim TJ, Ro JY. CD1d expressed in mast cell surface enhances IgE production in B cells by up-regulating CD40L expression and mediator release in allergic asthma in mice. *Cell Signal*. 2014;26(5):1105–1117.
16. Mekori YA, Metcalfe DD. Mast cell-T cell interactions. *J Allergy Clin Immunol*. 1999;104(3 Pt 1):517–523.
17. Vantourout P, Hayday A. Six-of-the-best: unique contributions of γδ T cells to immunology. *Nat Rev Immunol*. 2013;13(2):88–100.
18. Bonneville M, O'Brien RL, Born WK. Gammadelta T cell effector functions: a blend of innate programming and acquired plasticity. *Nat Rev Immunol*. 2010;10(7):467–478.
19. Wang T, et al. IFN-gamma-producing gamma delta T cells help control murine West Nile virus infection. *J Immunol*. 2003;171(5):2524–2531.
20. Wang T, et al. Gamma delta T cells facilitate adaptive immunity against West Nile virus infection in mice. *J Immunol*. 2006;177(3):1825–1832.
21. Jutila MA, Holderness J, Graff JC, Hedges JF. Antigen-independent priming: a transitional response of bovine gammadelta T-cells to infection. *Anim Health Res Rev*. 2008;9(1):47–57.
22. Reber LL, Marichal T, Galli SJ. New models for analyzing mast cell functions in vivo. *Trends Immunol*. 2012;33(12):613–625.
23. Bousso P. T-cell activation by dendritic cells in the lymph node: lessons from the movies. *Nat Rev Immunol*. 2008;8(9):675–684.
24. Dudeck A, et al. Mast cells are key promoters of contact allergy that mediate the adjuvant effects of haptens. *Immunity*. 2011;34(6):973–984.
25. Kohno M, Pouyssegur J. Targeting the ERK signaling pathway in cancer therapy. *Ann Med*. 2006;38(3):200–211.
26. Küsters-Vandevelde HV, et al. Experimental treatment of NRAS-mutated neurocutaneous melanocytosis with MEK162, a MEK-inhibitor. *Acta Neuropathol Commun*. 2014;2:41.
27. Willcox CR, et al. Cytomegalovirus and tumor stress surveillance by binding of a human γδ T cell antigen receptor to endothelial protein C receptor. *Nat Immunol*. 2012;13(9):872–879.
28. Itohara S, et al. T cell receptor delta gene mutant mice: independent generation of alpha beta T cells and programmed rearrangements of gamma delta TCR genes. *Cell*. 1993;72(3):337–348.
29. Ganusov VV, Pilyugin SS, de Boer RJ, Murali-Krishna K, Ahmed R, Antia R. Quantifying cell turnover using CFSE data. *J Immunol Methods*. 2005;298(1-2):183–200.
30. Carroll-Portillo A, et al. Mast cells and dendritic cells form synapses that facilitate antigen transfer for T cell activation. *J Cell Biol*. 2015;210(5):851–864.
31. Skokos D, et al. Mast cell-dependent B and T lymphocyte activation is mediated by the secretion of immunologically active exosomes. *J Immunol*. 2001;166(2):868–876.
32. Nakae S, Suto H, Kakurai M, Sedgwick JD, Tsai M, Galli SJ. Mast cells enhance T cell activation: Importance of mast cell-derived TNF. *Proc Natl Acad Sci U S A*. 2005;102(18):6467–6472.
33. Chiappori F, Merelli I, Milanesi L, Rovida E. Exploring the role of the phospholipid ligand in endothelial protein C receptor: a molecular dynamics study. *Proteins*. 2010;78(12):2679–2690.
34. Carnec X, et al. The Phosphatidylserine and Phosphatidylethanolamine Receptor CD300a Binds Dengue Virus and Enhances Infection. *J Virol*. 2016;90(1):92–102.
35. Tedla N, et al. Regulation of T lymphocyte trafficking into lymph nodes during an immune response by the chemokines macrophage inflammatory protein (MIP)-1 alpha and MIP-1 beta. *J Immunol*. 1998;161(10):5663–5672.
36. Kurashige C, Hashimoto T, Hatai B. Mast cells in the lymphnode sinus of the rat. *Arch Histol Jpn*. 1966;27(1):345–350.
37. St John AL. Influence of mast cells on dengue protective immunity and immune pathology. *PLoS Pathog*. 2013;9(12):e1003783.
38. Low JG, et al. Early Dengue infection and outcome study (EDEN) — study design and preliminary findings. *Ann Acad Med Singap*. 2006;35(11):783–789.
39. Schulze IT, Schlesinger RW. Plaque assay of dengue and other group B arthropod-borne viruses under methyl cellulose overlay media. *Virology*. 1963;19:40–48.
40. Zhang X, Goncalves R, Mosser DM. The isolation and characterization of murine macrophages. *Curr Protoc Immunol*. 2008;Chapter 14:Unit 14.1.
41. Madaan A, Verma R, Singh AT, Jain SK, Jaggi M. A stepwise procedure for isolation of murine bone marrow generation of dendritic cells. *J Biol Methods*. 2014;1(1):e1.